Analytical Solution of the Zero-Thickness Perfectly-Conducting Circular Disk in the Presence of an Axisymmetric Magnetic Dipole: A Second-Kind Fredholm Integral-Equation Approach

Luigi Verolino[1], Giampiero Lovat[2, *], Dario Assante[3], Amedeo Andreotti[1], Rodolfo Araneo[2], Paolo Burghignoli[4], and Salvatore Celozzi[2]

Abstract—The problem of radiation of a magnetic dipole axially symmetric with an infinitesimally thin perfectly conducting circular disk is solved in an exact closed form. This is done by transforming the original dual integral equation system describing the problem into a single second-kind Fredholm integral equation and searching for the solution as a power series. Both low- and high-frequency asymptotic limits are also discussed from which simple approximate solutions are readily derived. Numerical results are provided to validate the proposed formulation.

1. INTRODUCTION

The interaction of electromagnetic waves with a circular metal disk constitutes a classical diffraction problem that, along with its Babinet-complementary problem of diffraction by a circular hole in an infinite metal plate, has received considerable interest in the literature of the last decades (see, e.g., [1–20] and references therein).

Such a canonical configuration is in fact of interest for scattering (e.g., radar cross-section evaluation), antennas, as well as electromagnetic-shielding problems. Its electromagnetic features, in particular the presence of shape-dependent charge and current density distributions, also bear an interesting relation to the recently discovered optical resonances due to moving electric charges [21]. Limiting the discussion to time-harmonic regimes, different approaches have been proposed depending on the frequency range of interest (i.e., on the ratio between the wavelength of the incident wave and the involved dimensions of the scatterer), ranging from the classical Bethe theory for small holes to asymptotic high-frequency techniques such as the Physical Theory of Diffraction (PTD), Geometrical Theory of Diffraction (GTD), and derived methods. In the intermediate range, where the wavelength is comparable with the radius of the disk or of the aperture, numerical approaches are typically used; however, in order to alleviate the associated computational burden and also to gain physical insight into the involved solution, semi-analytical regularization techniques of various kinds have also been introduced.

In this paper we consider the incidence of spherical waves produced by a point source placed at a finite distance from a circular metallic disk, i.e., a Vertical Magnetic Dipole (VMD) placed along the axis (say, z) of azimuthal symmetry of the structure. This canonical source constitutes a valid representation for a practical electric-loop radiator parallel to the disk and co-axial with it, with radius small with respect to the operating wavelength.

Starting from the rigorous formulation of the problem in terms of a system of dual integral equations, different routes are illustrated to convert the system into a unique Fredholm integral equation of the second kind, whose favorable properties in connection with numerical discretization schemes are well known. The proposed approach is based on classical work on dual integral equations (see, e.g., [22–24]), also used in [25, 26] for a different problem involving point charges in uniform motion along the axis of circular holes. It allows for easily obtaining asymptotic approximations to the current induced on the disk valid either in the low- or in the high-frequency regimes, as well as a series representation of the exact solution valid at arbitrary frequencies.

The paper is organized as follows. In Section 2, the problem under analysis is formulated in terms of a system of dual integral equations in the unknown surface electric current density on the disk. In Section 3, this system is converted into suitable second-kind Fredholm integral equations, capable to provide asymptotic low- and high-frequency approximate solutions. In Section 4, a third transformation route is illustrated which allows for obtaining a general formulation valid at arbitrary frequencies, from which a representation of the unknown current density in terms of a power series in the ratio between the disk radius and the wavelength is derived. In Section 5, numerical results that check the accuracy and computational performance of the proposed formulation are provided. Finally, in Section 6 some conclusive remarks are given.

2. FORMULATION OF THE PROBLEM

The configuration under analysis consists of an infinitely thin, perfectly conducting (PEC) circular disk of radius a placed on the plane $z = 0$ of a Cartesian coordinate system (x, y, z) with center at the origin and a vertical magnetic dipole (VMD) with magnetic dipole moment m_z placed along the z axis at a height $z = h$ (see Fig. 1). Time-harmonic sources and fields are assumed with an implicit $e^{j\omega t}$ dependence.
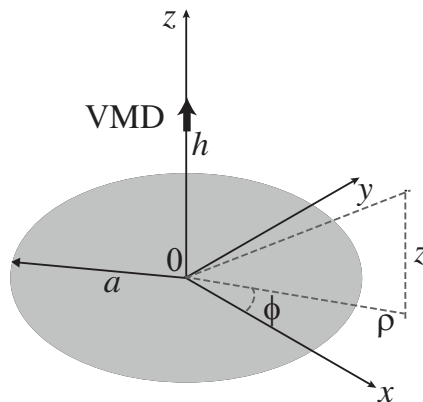

Figure 1. Configuration under analysis: an infinitely thin, perfectly conducting (PEC) circular disk of radius a placed on the plane $z = 0$ of a Cartesian coordinate system (x, y, z) with center at the origin and a vertical magnetic dipole (VMD) placed along the z axis at a height $z = h$.

2.1. Incident Field

As is well known, the vector potential and electromagnetic field associated with a VMD in free space can be expressed in a spherical coordinate system (r, ϕ, θ) centered in the VMD as [27]

$$A_\phi^0 (r, \theta) = -\frac{m_z}{4\pi} \left(\frac{1}{r^2} + \frac{jk_0}{r} \right) \sin\theta \, e^{-jk_0 r} \tag{1}$$

$$E_\phi^0 (r, \theta) = \frac{\zeta_0 m_z}{4\pi} \left[\frac{jk_0}{r^2} + \frac{(jk_0)^2}{r} \right] \sin\theta \, e^{-jk_0 r} \tag{2}$$

$$H_r^0(r, \theta) = -\frac{m_z}{2\pi} \left(\frac{1}{r^3} + \frac{jk_0}{r^2} \right) \cos\theta \, e^{-jk_0 r} \tag{3}$$

$$H_z^0(r, \theta) = -\frac{m_z}{4\pi} \left[\frac{1}{r^3} + \frac{jk_0}{r^2} + \frac{(jk_0)^2}{r} \right] \sin\theta \, e^{-jk_0 r} \tag{4}$$

where k_0 and ζ_0 are the free-space wavenumber and characteristic impedance, respectively.

However, due to the geometry of the problem under investigation, it is more convenient to express the above fields in a cylindrical coordinate system (ρ, ϕ, z), with a trivial change of variables.

2.2. Scattered Field

In the presence of the PEC disk, because of the symmetry of the configuration, the electric current density $\boldsymbol{J}$ induced on the disk is azimuthally directed and independent of the coordinate ϕ and can thus be expressed as

$$\boldsymbol{J}(\rho, z) = J_{S\phi}(\rho)\delta(z)\hat{\boldsymbol{\phi}} \tag{5}$$

where $\delta(\cdot)$ indicates the Dirac delta distribution.

It is then convenient to introduce the following Hankel-transform pair [28]:

$$\tilde{F}(\lambda) = \int_0^\infty \rho F(\rho) J_1(\lambda\rho) \mathrm{d}\rho \qquad F(\rho) = \int_0^\infty \lambda \tilde{F}(\lambda) J_1(\lambda\rho) \mathrm{d}\lambda \tag{6}$$

where $J_1(\cdot)$ is the first-kind Bessel function of order 1.

Therefore, the scattered vector potential and fields associated with the current distribution (5) are also independent of the variable ϕ and can be expressed as

$$A_\phi^{\mathrm{s}}(\rho, z) = -\frac{1}{2} \int_0^\infty \tilde{J}_{S\phi}(\lambda) \frac{e^{-|z|\sqrt{\lambda^2 - k_0^2}}}{\sqrt{\lambda^2 - k_0^2}} J_1(\lambda\rho) \lambda \mathrm{d}\lambda \tag{7}$$

$$E_\phi^{\mathrm{s}}(\rho, z) = \frac{jk_0\zeta_0}{2} \int_0^\infty \tilde{J}_{S\phi}(\lambda) \frac{e^{-|z|\sqrt{\lambda^2 - k_0^2}}}{\sqrt{\lambda^2 - k_0^2}} J_1(\lambda\rho) \lambda \mathrm{d}\lambda \tag{8}$$

$$H_\rho^{\mathrm{s}}(\rho, z) = -\mathrm{sign}(z) \frac{1}{2} \int_0^\infty \tilde{J}_{S\phi}(\lambda) e^{-|z|\sqrt{\lambda^2 - k_0^2}} J_1(\lambda\rho) \lambda \mathrm{d}\lambda \tag{9}$$

$$H_z^{\mathrm{s}}(\rho, z) = -\frac{1}{2} \int_0^\infty \tilde{J}_{S\phi}(\lambda) \frac{e^{-|z|\sqrt{\lambda^2 - k_0^2}}}{\sqrt{\lambda^2 - k_0^2}} J_0(\lambda\rho) \lambda^2 \mathrm{d}\lambda \tag{10}$$

where $\tilde{J}_{S\phi}(\lambda)$ is the Hankel transform (6) of the induced current density, $\mathrm{sign}(\cdot)$ the sign function, and $J_0(\cdot)$ the first-kind Bessel function of order 0.

2.3. Dual Integral Equations

In order to evaluate the unknown current density, it is necessary to enforce the appropriate boundary condition on the disk, i.e., that the total tangential electric field vanishes. From Eq. (8), with some trivial manipulations it is possible to obtain

$$\begin{aligned} \int_0^\infty \frac{\tilde{J}_{S\phi}(\lambda)}{\sqrt{\lambda^2 - k_0^2}} J_1(\lambda\rho) \lambda \mathrm{d}\lambda &= -\frac{2}{jk_0\zeta_0} E_\phi^0(\rho, z = -h) \quad \rho < a \\ \int_0^\infty \tilde{J}_{S\phi}(\lambda) J_1(\lambda\rho) \lambda \mathrm{d}\lambda &= 0 \qquad\qquad\qquad\qquad\quad \rho > a \end{aligned} \tag{11}$$

where E_ϕ^0 indicates the ϕ-component of the incident electric field, and the second equation in Eq. (11) expresses the fact that the current density vanishes outside the disk. Equation (11) constitutes a system of dual integral equations.

In addition, the presence of a sharp PEC edge at $\rho = a$ entails a singular behavior of the current density in the proximity of the edge [29], i.e.,

$$\lim_{\rho \to a} \sqrt{a^2 - \rho^2} \, J_{S\phi}(\rho) \to \text{finite value} \tag{12}$$

Several techniques allow for solving the system in Eq. (11). In particular, several transformations allow to express the system of integral equations as a single Fredholm integral equation of second kind. In the next sections some of these techniques will be discussed.

3. ASYMPTOTIC HIGH- AND LOW-FREQUENCY SOLUTIONS

3.1. High-Frequency Transformation

In order to find an asymptotic high-frequency solution for the current density, it is useful to turn the dual system of integral Equation (11) into a Fredholm integral equation of the second kind. To this aim, one can observe that the system (11) is equivalent to the following equation:

$$\int_0^\infty \lambda \tilde{J}_{S\phi}(\lambda) J_1(\lambda v) \, \mathrm{d}\lambda = u(a-v) \left[\frac{2C}{jk_0\zeta_0} E_\phi^0(v,-h) + \int_0^\infty \lambda \tilde{J}_{S\phi}(\lambda) \left(1 - \frac{C}{\sqrt{\lambda^2 - k_0^2}} \right) J_1(\lambda v) \, \mathrm{d}\lambda \right] \tag{13}$$

where C is an arbitrary constant (with the dimension of a propagation constant); $u(\cdot)$ is the unit-step Heaviside function; and the variable v has been used instead of ρ for further convenience. By Hankel transforming both sides of Eq. (13), one obtains

$$\tilde{J}_{S\phi}(w) = -\frac{2C}{jk_0\zeta_0} \int_0^a v J_1(wv) E_\phi^0(v,-h) \mathrm{d}v + \int_0^\infty \lambda \tilde{J}_{S\phi}(\lambda) \left(1 - \frac{C}{\sqrt{\lambda^2 - k_0^2}} \right) M(w,\lambda) \, \mathrm{d}\lambda \tag{14}$$

having used the well-known completeness relation [30]

$$\int_0^\infty v J_1(\lambda v) J_1(wv) \, \mathrm{d}v = \frac{\delta(w-\lambda)}{\lambda} \tag{15}$$

and having defined

$$M(w,\lambda) = \int_0^a v J_1(\lambda v) J_1(wv) \, \mathrm{d}v = \frac{a^2 w \lambda}{2} \frac{J_0(\lambda a) J_2(wa) - J_0(wa) J_2(\lambda a)}{w^2 - \lambda^2} \tag{16}$$

The fact that $M(w,\lambda)$ is a symmetric function (i.e., it is possible to exchange w and λ) helps to make numerical methods stable.

It is worth noting that the constant C may assume any complex value. The best choice is to assume $C = jk_0$, since in this way the second integral in Eq. (14) vanishes for $k_0 \to \infty$. Therefore, at high frequencies it results

$$\tilde{J}_{S\phi}(w) \simeq -\frac{2}{\zeta_0} \int_0^a v J_1(wv) E_\phi^0(v,-h) \mathrm{d}v \tag{17}$$

By inverse Hankel transforming (17), it is possible to finally obtain

$$J_{S\phi}(\rho) \simeq -\frac{2}{\zeta_0} E_\phi^0(\rho,-h) = -\frac{m_z}{2\pi} \left[\frac{jk_0}{(\rho^2 + h^2)^{3/2}} + \frac{(jk_0)^2}{\rho^2 + h^2} \right] \rho \, e^{-jk_0\sqrt{\rho^2+h^2}} \tag{18}$$

This high-frequency asymptotic solution does not satisfy the boundary condition (12), since such a behavior has been lost by neglecting the kernel in the integral equation. Moreover, in the asymptotic limit $k_0 a \gg 1$ the disk tends to be infinite, the edge tends to disappear and, therefore, the proposed approximation does not include Meixner's condition (12).

It is worth noting that Eq. (18) could also be obtained by directly observing that the system in Eq. (11), in the limit $a \to \infty$, would simply reduce to the first equation which, in turn, could be inverted by means of a simple Hankel transform. However, the proposed transformation leads to the integral equation (14) which can be used not only to find an asymptotic high-frequency solution, but, more in general, to compute the solution in a broader range of frequencies, e.g., by means of a fixed-point iterative method.

3.2. Low-frequency Transformation

Let us now consider the opposite low-frequency asymptotic limit $k_0 \to 0$. To this aim, it is convenient to transform the kernel of Eq. (11) into a trigonometric one. In particular, by using the following representation of the Bessel function J_1:

$$J_1(\lambda\rho) = \frac{2}{\pi\rho} \int_0^\rho \frac{x \sin(\lambda x)}{\sqrt{\rho^2 - x^2}} dx \tag{19}$$

inserting it in the first of Eq. (11), exchanging the order of integrations, and performing an inverse Abel transform, the first of Eq. (11) becomes

$$\int_0^\infty \frac{\tilde{J}_{S\phi}(\lambda)}{\sqrt{\lambda^2 - k_0^2}} \sin(\lambda x) \lambda d\lambda = \hat{J}_\phi^0(x, -h) \tag{20}$$

where, for the sake of simplicity, we have introduced

$$\hat{J}_\phi^0(x, -h) = -\frac{2\pi}{jk_0\zeta_0} A_4^{-1} \left\{ \rho E_\phi^0(\rho, -h) \right\} \tag{21}$$

with $A_4^{-1} \{\cdot\}$ being the inverse Abel transform of fourth type [31], whose general definition is

$$\hat{f}(r) = A_4 \{f(x)\} = 2 \int_0^r \frac{x f(x)}{(r^2 - x^2)^{1/2}} dx$$

$$f(x) = A_4^{-1} \left\{ \hat{f}(r) \right\} = \frac{\hat{f}(0)}{\pi x} + \frac{1}{\pi} \int_0^x \frac{f'(r)}{(x^2 - r^2)^{1/2}} dr \tag{22}$$

For the second of Eq. (11) it is sufficient to use the integral [26]

$$\int_x^\infty \frac{J_1(u\rho)}{\sqrt{\rho^2 - x^2}} d\rho = \frac{\sin(ux)}{ux} \tag{23}$$

so that the system of dual integral Equation (11) becomes

$$\int_0^\infty \frac{\tilde{J}_{S\phi}(\lambda)}{\sqrt{\lambda^2 - k_0^2}} \sin(\lambda x) \lambda d\lambda = \hat{J}_\phi^0(x, -h) \quad x < a$$

$$\int_0^\infty \tilde{J}_{S\phi}(\lambda) \sin(\lambda x) d\lambda = 0 \qquad x > a \tag{24}$$

By adopting a technique similar to that used in the previous subsection, the system in Eq. (24) can be reduced to a single integral equation as

$$\int_0^\infty \tilde{J}_{S\Phi}(w) \sin(wx) dw = u(a - x) \left[\hat{J}_\phi^0(x, -h) + \int_0^\infty \left(1 - \frac{w}{\sqrt{w^2 - k_0^2}} \right) \tilde{J}_{S\Phi}(w) \sin(wx) dw \right] \tag{25}$$

By recalling that

$$\int_0^\infty \sin(\lambda x) \sin(wx) dx = \frac{\pi}{2} \left[\delta(\lambda - w) - \delta(\lambda + w) \right] \tag{26}$$

and introducing the function

$$N(w, \lambda) = \int_0^a \sin(wx) \sin(\lambda x) dx = \frac{w \sin(\lambda a) \cos(wa) - \lambda \cos(\lambda a) \sin(wa)}{\lambda^2 - w^2} \tag{27}$$

Eq. (25) can be rewritten as a Fredholm integral equation of second kind as

$$\tilde{J}_{S\Phi}(\lambda) = \frac{2}{\pi} \int_0^a \hat{J}_\phi^0(x, -h) \sin(\lambda x) dx + \frac{2}{\pi} \int_0^\infty \left(1 - \frac{w}{\sqrt{w^2 - k_0^2}} \right) \tilde{J}_{S\Phi}(w) N(w, \lambda) dw \tag{28}$$

It is worth noting that $N(w, \lambda)$ is a symmetric function. The integral equation (28) is equivalent to Eq. (14), but it is more suitable for low-frequency considerations. In fact, for $k_0 \to 0$ the second integral in Eq. (28) vanishes, so that the low-frequency solution of the problem is

$$\tilde{J}_{S\Phi}(\lambda) \simeq \frac{2}{\pi} \int_0^a \hat{J}_\phi^0(x, -h) \sin(\lambda x) \, dx \tag{29}$$

By inverse Hankel transforming Eq. (29), after some manipulations one finally obtains

$$J_{S\phi}(\rho) \simeq \frac{2}{\pi} \int_0^\infty \lambda \left(\int_0^a \hat{J}_\phi^0(x, -h) \sin(\lambda x) \, dx \right) J_1(\lambda \rho) d\lambda$$

$$= \frac{2}{\pi} \left[\frac{\rho \hat{J}_\phi^0(a, -h)}{\sqrt{a^2 - \rho^2} \left(a + \sqrt{a^2 - \rho^2} \right)} + \frac{\hat{J}_\phi^0(\rho, -h)}{\rho} - \int_\rho^a \frac{\rho \hat{J}_\phi^{0\prime}(x, -h)}{\sqrt{x^2 - \rho^2} \left(x + \sqrt{x^2 - \rho^2} \right)} dx \right] \tag{30}$$

where $\hat{J}_\phi^{0\prime}(x, -h)$ indicates the first derivative of $\hat{J}_\phi^0(x, -h)$.

Equation (30) represents the generic low-frequency solution of the problem under consideration. It is worth noting that the first term in Eq. (30) exhibits the expected boundary divergence (12). The second term tends to be a finite value as ρ tends to be zero, since $\hat{J}_\phi^0(0, -h)$ is $O(\rho)$ in this limit. Finally, the last term is a regular and quickly convergent integral.

With reference to the considered source, the electric field produced by the VMD is

$$E_\phi^0(x, -h) = \frac{m_z \zeta_0}{4\pi} \left[\frac{jk_0}{(x^2 + h^2)^{3/2}} + \frac{(jk_0)^2}{x^2 + h^2} \right] x \, e^{-jk_0 \sqrt{x^2 + h^2}} \tag{31}$$

which can be approximated at low frequencies as

$$E_\phi^0(\rho, -h) \simeq \frac{jk_0 m_z \zeta_0}{4\pi} \frac{\rho}{(\rho^2 + h^2)^{3/2}} \tag{32}$$

From Eqs. (21), (22), and (32), the function $\hat{J}_\phi^0(x, -h)$ can thus be approximated as

$$\hat{J}_\phi^0(x, -h) \simeq -\frac{m_z}{2\pi} \int_0^x \frac{\rho}{\sqrt{x^2 - \rho^2}} \frac{2h^2 - \rho^2}{(\rho^2 + h^2)^{5/2}} d\rho = -\frac{m_z}{\pi} \frac{hx}{(h^2 + x^2)^2} \tag{33}$$

which can be used in Eq. (30) to obtain the sought low-frequency solution.

4. SOLUTION OF THE PROBLEM

In the previous section, the system of dual integral Equation (11) has been turned into different single Fredholm integral equations of second kind (e.g., Eqs. (14) and (28)), whose numerical discretization formally solves the problem for any frequency of interest. However, the involved integrals extend over an infinite domain and have oscillating integrands, hence their computation may be numerically troublesome. In this section we present an alternative method for turning the system of dual integral equations into a single Fredholm second-kind integral equation, involving integrals extended on *finite* domains.

To this aim, it is convenient to represent the induced surface current density as

$$\tilde{J}_{S\Phi}(\lambda) = \int_0^a q(y, k_0) \sin(\lambda y) \, dy \tag{34}$$

where $q(y, k_0)$ is an unknown auxiliary function, continuous with its first derivative in the interval $[0, a] \times [0, +\infty]$, i.e., $q \in C^1([0, a] \times [0, +\infty])$. It is worth noting that, since Eq. (34) has the same functional form of Eq. (29), the expression of the induced current density adopting such a representation has the same functional form of Eq. (30), i.e.,

$$J_{S\phi}(\rho) = \frac{\rho \, q(a, k_0)}{\sqrt{a^2 - \rho^2} \left(a + \sqrt{a^2 - \rho^2} \right)} + \frac{q(\rho, k_0)}{\rho} - \int_\rho^a \frac{\rho}{\sqrt{y^2 - \rho^2} \left(y + \sqrt{y^2 - \rho^2} \right)} \frac{\partial q(y, k_0)}{\partial y} dy \tag{35}$$

However, there is a fundamental difference between the two expressions. In fact, while Eq. (30) is a low-frequency approximation, Eq. (35) is valid for arbitrary frequencies, due to the presence of the frequency-dependent function $q(y, k_0)$. However, they coincide in the low-frequency limit, as it will be verified later on in this section.

By observing the first term in Eq. (35), it is clear that the proposed representation automatically satisfies the edge condition. Moreover, Eq. (35) does not present any singularity at the origin, as expected, since the second term for $\rho \to 0$ approaches $\partial q / \partial y (y = 0, k_0)$, which is finite since $q(y, k_0) \in C^1$.

In addition, by multiplying Eq. (34) by $\sin(\lambda x)$, integrating over $[0, +\infty]$, and using Eq. (26) with $\lambda \to x$, $w \to y$, and $x \to \lambda$, the second equation in Eq. (24) is automatically satisfied. On the other hand, the first equation in Eq. (24) becomes

$$\int_0^\infty \int_0^a \frac{\lambda q(y, k_0)}{\sqrt{\lambda^2 - k_0^2}} \sin(\lambda y) \sin(\lambda x) \, dy d\lambda = \hat{J}_\phi^0(x, -h) \tag{36}$$

The latter can also be written as

$$\int_0^\infty \int_0^a q(y, k_0) \sin(\lambda y) \sin(\lambda x) \, dy d\lambda + \int_0^\infty \int_0^a q(y, k_0) \left(\frac{\lambda}{\sqrt{\lambda^2 - k_0^2}} - 1 \right) \sin(\lambda y) \sin(\lambda x) \, dy d\lambda$$
$$= \hat{J}_\phi^0(x, -h) \tag{37}$$

Taking into account the identity in Eq. (26), Eq. (37) can be rewritten as

$$\frac{\pi}{2} q(x, k_0) = \hat{J}_\phi^0(x, -h) + \int_0^\infty \int_0^a q(y, k_0) \left(1 - \frac{\lambda}{\sqrt{\lambda^2 - k_0^2}} \right) \sin(\lambda y) \sin(\lambda x) \, dy d\lambda \tag{38}$$

so that the following second-kind Fredholm integral equation is obtained:

$$q(x, k_0) = T(x) + \frac{k_0}{2} \int_0^a \{ G[k_0(y - x)] - G[k_0(y + x)] \} q(y, k_0) \, dy \tag{39}$$

where

$$T(x) = \frac{2}{\pi} \hat{J}_\phi^0(x, -h) \tag{40}$$

while the kernel is

$$G(t) = \frac{2}{\pi} \int_0^\infty \left(1 - \frac{v}{\sqrt{v^2 - 1}} \right) \cos(vt) \, dv \tag{41}$$

It is worth noting that, in the asymptotic low-frequency limit $k_0 a \to 0$, the integral in Eq. (39) vanishes so that, in such a limit, $q(x, 0) \simeq T(x)$. Therefore, as anticipated in the introduction of the section, in the low-frequency limit the functions $q(x, k_0)$ and $\hat{J}_\phi^0(x, -h)$ become proportional, and Eqs. (30) and (35) coincide.

More in general, it is possible to represent the function $q(\cdot)$ as a power series of $(k_0 a)$, i.e.,

$$q(\rho, k_0) = \sum_{n=0}^\infty q_n(\rho)(k_0 a)^n \tag{42}$$

Similarly, it is possible to represent the functions $T(\cdot)$ and $G(\cdot)$ as

$$T(\rho, k_0) = \sum_{n=0}^\infty T_n(\rho)(k_0 a)^n \qquad G(t) = \sum_{n=0}^\infty G_n |t|^n \tag{43}$$

By inserting such representations into Eq. (39) and using the Cauchy product of two power series, it is easy to obtain the following recurrence equation:

$$q_n(\rho) = T_n(\rho) + \frac{1}{2} \sum_{m=1}^{n-1} \frac{G_m}{a^{m+1}} \int_0^a \left[|y - \rho|^m - (y + \rho)^m \right] q_{n-m-1}(y) \, dy \tag{44}$$

for $n > 0$ and $q_0(\rho) = T_0(\rho)$. It is worth noting that the coefficients $T_n(\rho)$ and G_m can be computed analytically, as shown in Appendix A (see Eqs. (A4), (A11), and (A20)-(A21)). In particular, it is found that

$$q_0(\rho) = T_0(\rho) = -\frac{2m_z}{\pi^2}\frac{h\rho}{(h^2 + \rho^2)^2} \qquad (45)$$

Moreover $q_1(\rho) = T_1(\rho) = 0$ and

$$q_2(\rho) = -\frac{m_z h}{2\pi^2 a^2}\left(\frac{1}{\rho^2 + h^2} + \frac{1}{a^2 + h^2}\right)\rho \qquad (46)$$

$$q_3(\rho) = j\frac{4m_z\rho}{3\pi^3(a^2 + h^2)a^3}\left[ah + (a^2 + h^2)\left(\frac{\pi}{2} - \tan^{-1}\frac{a}{h}\right)\right] \qquad (47)$$

$$q_4(\rho) = \frac{m_z h\rho}{48\pi^2(a^2 + h^2)a^4}\left[(27a^2 + 12h^2 + r^2) + 3(a^2 + h^2)\log\left(\frac{\rho^2 + h^2}{a + h^2}\right)\right] \qquad (48)$$

The higher-order terms q_n can also be calculated analytically through Eqs. (44), (A4), (A11), and (A20)–(A21). The expressions for the odd terms q_{2n+1} involve terms of the kind ρ^k ($k = 0, \ldots, 2n - 1$). The expressions for the even terms q_{2n} involve terms of the kind ρ^k ($k = 0, \ldots, 2n - 1$) and $\rho(\rho^2 + h^2)^{n-2}\log(\rho^2 + h^2)$. However, for $n > 4$ the expressions are quite involute and not reported here for brevity. Once the coefficients $q_n(\rho)$ (and hence the function $q(\rho, k_0)$) are known, the current $J_{S\Phi}(\rho)$ can be obtained through Eq. (35).

5. NUMERICAL RESULTS

To check the validity and accuracy of the proposed formulations, a case study is presented here, i.e., a VMD placed at $z = h = 50\,\text{cm}$ over a PEC disk with radius $a = 5\,\text{cm}$. The current-density profile obtained through Eqs. (35) (*Proposed analytical solution*), (30) (*Low-frequency solution*), and (18) (*High-frequency solution*) is reported as a function of ρ/a for different frequencies (Figs. 2–6) and compared with numerical results obtained through a conventional Method-of-Moment (MoM) solution with entire-domain basis functions (*Exact (MoM)*) [18].
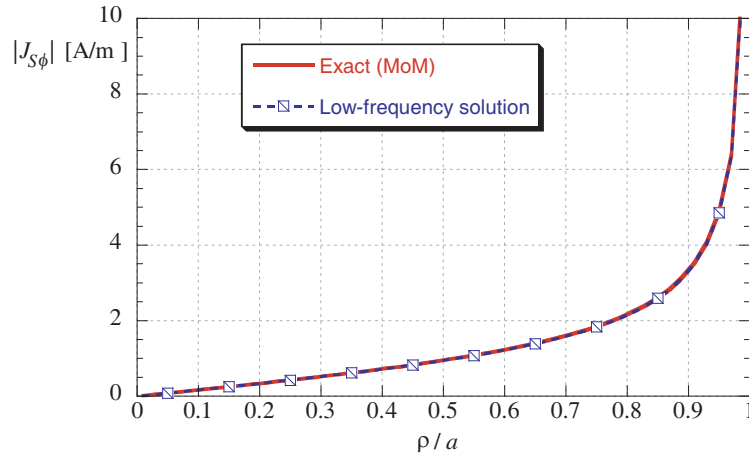

Figure 2. Surface current density as a function of ρ/a for $k_0 a = 0.01$ with $a = 5\,\text{cm}$, i.e., $f = 9.54\,\text{MHz}$. *Parameters*: $h = 50\,\text{cm}$, $m_z = 1\,\text{Am}^2$.

In Fig. 2, the comparison is shown for $k_0 a = 0.01$ (i.e., $f = 9.54\,\text{MHz}$) between the exact numerical MoM results and the proposed low-frequency solution (which also considers only one term in the proposed analytical formulation). As can be seen, the curves are perfectly superimposed. On the other hand, for $k_0 a = 0.1$ (i.e., $f = 95.4\,\text{MHz}$), the exact solution starts to deviate from its low-frequency
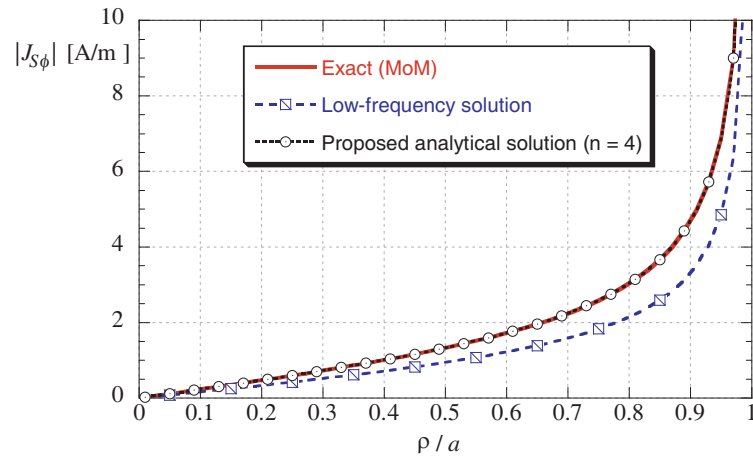
Figure 3. Surface current density as a function of ρ/a for $k_0 a = 0.1$ with $a = 5\,\mathrm{cm}$, i.e., $f = 95.4\,\mathrm{MHz}$. *Parameters*: $h = 50\,\mathrm{cm}$, $m_z = 1\,\mathrm{Am^2}$.
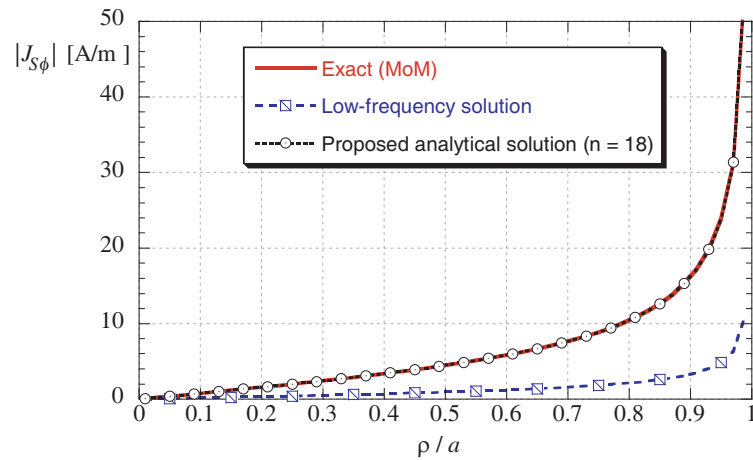
Figure 4. Surface current density as a function of ρ/a for $k_0 a = 0.5$ with $a = 5\,\mathrm{cm}$, i.e., $f = 0.48\,\mathrm{GHz}$. *Parameters*: $h = 50\,\mathrm{cm}$, $m_z = 1\,\mathrm{Am^2}$.
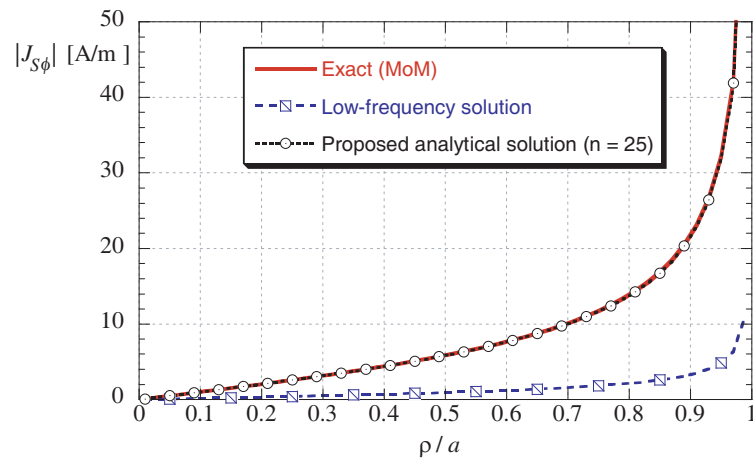
Figure 5. Surface current density as a function of ρ/a for $k_0 a = 0.7$ with $a = 5\,\mathrm{cm}$, i.e., $f = 0.67\,\mathrm{GHz}$. *Parameters*: $h = 50\,\mathrm{cm}$, $m_z = 1\,\mathrm{Am^2}$.
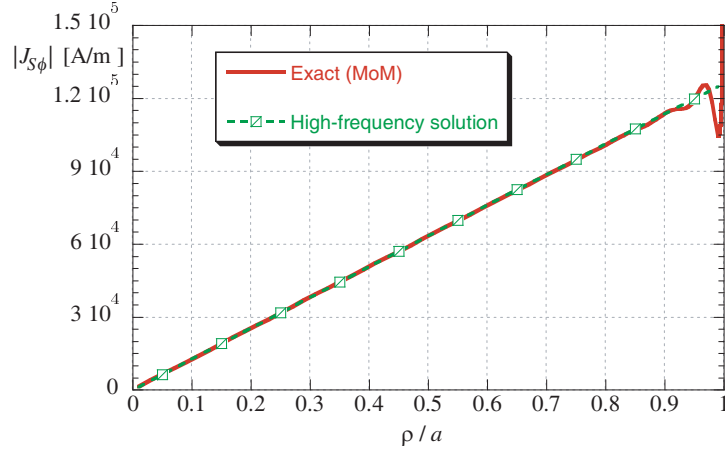
Figure 6. Surface current density as a function of ρ/a for $k_0 a = 100$ with $a = 5\,\text{cm}$, i.e., $f = 95.4\,\text{GHz}$. *Parameters*: $h = 50\,\text{cm}$, $m_z = 1\,\text{Am}^2$.

Figure 7. Surface current density as a function of frequency f for $\rho/a = 0.25$. *Parameters*: $h = 50\,\text{cm}$, $a = 5\,\text{cm}$, $m_z = 1\,\text{Am}^2$.

approximation, while the proposed analytical solution is correct by taking $n = 4$ terms in the power expansion of the q function (i.e., in Eq. (42)), as it can be seen in Fig. 3. By increasing frequency (i.e., by increasing $k_0 a$), more terms are needed in the expression of the q function to correctly reproduce the exact behavior of the surface current density, as it can be seen in Figs. 4 and 5 where the results correspond to the cases $k_0 a = 0.5$ (i.e., $f = 480\,\text{MHz}$) and $k_0 a = 0.7$ (i.e., $f = 670\,\text{MHz}$) and where $n = 18$ and $n = 25$ terms are used, respectively. Finally, the high-frequency case $k_0 a = 100$ (i.e., $f = 95.4\,\text{GHz}$) is reported in Fig. 6 where, as expected, the simple high-frequency solution in Eq. (18) is perfectly superimposed to the exact numerical MoM solution, except very close to the edge $\rho/a = 1$. In this case, the exact MoM result presents slight oscillations starting from $\rho/a \simeq 0.84$ and starts to increase monotonically towards infinity from $\rho/a = 0.993$.

The comparison among all the formulations for the surface-current density as a function of the product $k_0 a$ is instead reported in Figs. 7–9 for $\rho/a = 0.25$, $\rho/a = 0.5$, and $\rho/a = 0.75$, respectively, to point out the limits of the low- and high-frequency solutions. The proposed analytical solution is always perfectly superimposed to the exact numerical MoM results, provided that a sufficient number of terms are considered in the series expansion of the q function. As can be seen, the low-frequency solution is a good approximation up to $k_0 a \simeq 0.08$ (i.e., $f = 76.3\,\text{MHz}$) while the high-frequency solution starts to correctly reproduce the exact surface current behavior from $k_0 a \simeq 5$ (i.e., $f = 4.77\,\text{GHz}$).
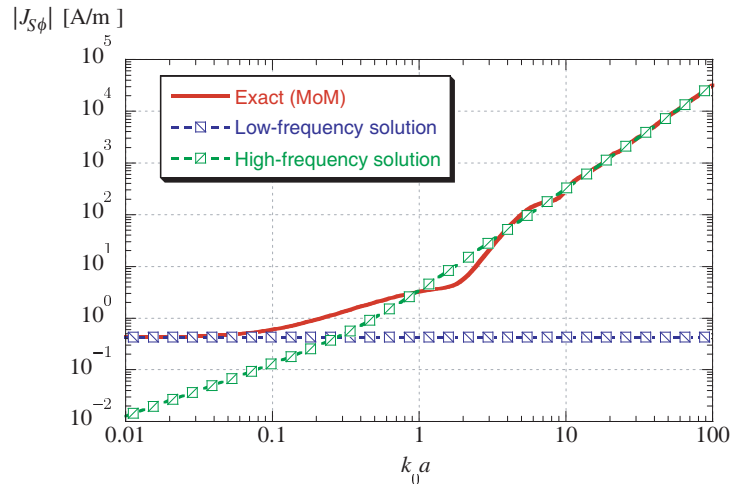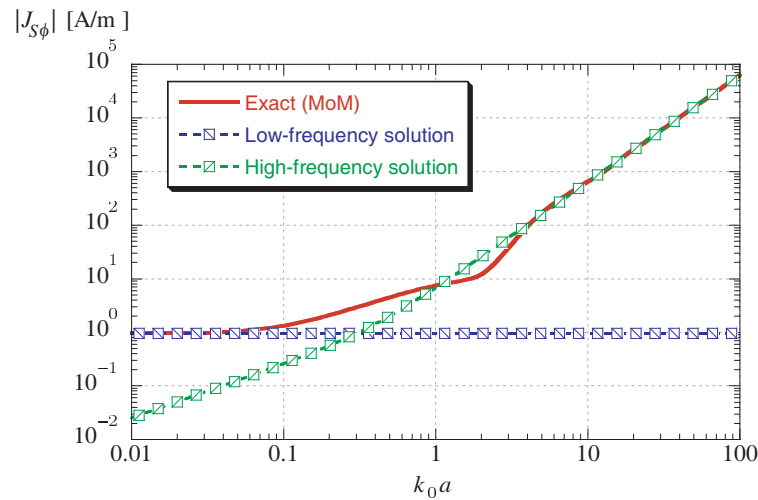
Figure 8. Surface current density as a function of frequency f for $\rho/a = 0.5$. *Parameters*: $h = 50$ cm, $a = 5$ cm, $m_z = 1$ Am^2.
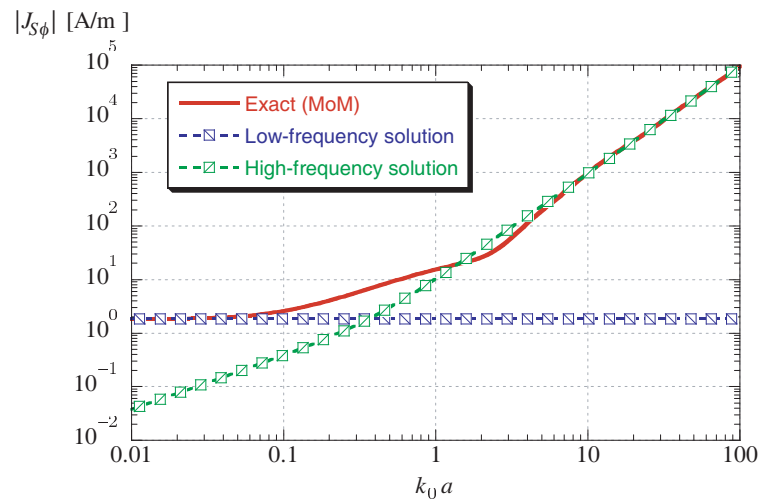

Figure 9. Surface current density as a function of frequency f for $\rho/a = 0.75$. *Parameters*: $h = 50$ cm, $a = 5$ cm, $m_z = 1$ Am^2.

6. CONCLUSION

The problem of an infinitesimally thin perfectly conducting circular disk excited by an axially symmetric magnetic dipole has been addressed. The problem has been first formulated in terms of a system of dual integral equations which has been converted in different second-kind Fredholm integral equations amenable to different asymptotic low- and high-frequency solutions in closed form. An exact analytical solution valid at arbitrary frequencies is also obtained in terms of a power series. Numerical results are provided to validate the accuracy and the limits of the proposed solutions. In summary, the considered problem has been solved successfully at all frequencies: the low-and high-frequency ranges are covered by the approximate formulations; these are not accurate in the intermediate range, where the exact formulation can instead be used.

APPENDIX A. SERIES REPRESENTATIONS OF THE FUNCTIONS G AND T

The integral (41) can be solved in a closed form. In fact [32, 3.771.12–3.771.13]

$$
\begin{aligned}
G\left(t\right) &= \frac{2}{\pi}\left\{\int_0^1\left(1+j\frac{v}{\sqrt{1-v^2}}\right)\cos\left(vt\right)\mathrm{d}v + \int_1^\infty\left(1-\frac{v}{\sqrt{v^2-1}}\right)\cos\left(vt\right)\mathrm{d}v\right\} \\
&= \frac{2}{\pi}\left\{\frac{\sin t}{t}+j\frac{\pi}{2}\mathbf{H}_{-1}\left(|t|\right)+\frac{\pi}{2}J_1\left(|t|\right)-\frac{\sin|t|}{|t|}\right\} \\
&= J_1\left(|t|\right)+j\mathbf{H}_{-1}\left(|t|\right)
\end{aligned}
\tag{A1}
$$

where $\mathbf{H}_{-1}\left(\cdot\right)$ is the Struve function of order -1 [32, 8.55].

The series expansion of the G function can thus be obtained through the series expansions of the Bessel and Struve functions [32, 8.441.2–8.550]. From Eq. (A1) we thus have

$$
G\left(t\right) = \sum_{m=0}^\infty \left(-1\right)^m\frac{|t|^{2m+1}}{2^{2m+1}m!\left(m+1\right)!} + j\sum_{m=0}^\infty \left(-1\right)^m\frac{|t|^{2m}}{2^{2m}\Gamma\left(m+3/2\right)\Gamma\left(m+1/2\right)}
\tag{A2}
$$

i.e.,

$$
G\left(t\right) = \sum_{n=0}^\infty G_n|t|^n
\tag{A3}
$$

with

$$
G_n = \begin{cases}
j\dfrac{\left(-1\right)^{n/2}}{2^n\Gamma\left(\dfrac{n+3}{2}\right)\Gamma\left(\dfrac{n+1}{2}\right)} & n\text{ even} \\[4ex]
\dfrac{\left(-1\right)^{\frac{n-1}{2}}}{2^n\left(\dfrac{n-1}{2}\right)!\left(\dfrac{n+1}{2}\right)!} & n\text{ odd}
\end{cases}
\tag{A4}
$$

By considering the complete expression of the electric field $E_\phi^0(\rho,-h)$, it is not possible to find a closed-form expression for the function

$$
T\left(\rho\right) = \frac{2}{\pi}\hat{J}_\phi^0\left(\rho,-h\right) = -\frac{4}{j\pi k_0\zeta_0}\int_0^\rho\frac{\partial}{\partial r}\left[rE_\phi^0\left(r,-h\right)\right]\frac{1}{\sqrt{\rho^2-r^2}}\mathrm{d}r
\tag{A5}
$$

Therefore we assume the general representation

$$
T\left(\rho\right) = \sum_{n=0}^\infty T_n\left(\rho\right)\left(k_0a\right)^n
\tag{A6}
$$

In order to compute all the coefficients of the series, we start from (A5), using (31), together with the series expansion of the exponential function so that

$$
\begin{aligned}
xE_\phi^0\left(x,-h\right) &= \frac{m_z\zeta_0}{4\pi}\left[\frac{jk_0}{\left(x^2+h^2\right)^{3/2}}+\frac{\left(jk_0\right)^2}{x^2+h^2}\right]x^2\,e^{-jk_0\sqrt{x^2+h^2}} \\
&= \frac{m_z\zeta_0}{4\pi}\left[\frac{jk_0}{\left(x^2+h^2\right)^{3/2}}+\frac{\left(jk_0\right)^2}{x^2+h^2}\right]x^2\sum_{n=0}^\infty\frac{\left(-jk_0\right)^n\left(x^2+h^2\right)^{\frac{n}{2}}}{n!} \\
&= \frac{m_z\zeta_0x^2}{4\pi}\left[jk_0\left(x^2+h^2\right)^{-3/2}+\sum_{n=0}^\infty\frac{\left(-jk_0\right)^{n+3}\left(n+1\right)}{\left(n+2\right)!}\left(x^2+h^2\right)^{\frac{n-1}{2}}\right]
\end{aligned}
\tag{A7}
$$

and

$$
\frac{\partial}{\partial x}\left[xE_\phi^0\left(x,-h\right)\right] = \frac{m_z\zeta_0x}{4\pi}\left\{jk_0\frac{2h^2-x^2}{\left(x^2+h^2\right)^{5/2}}+\sum_{n=0}^\infty\frac{\left(-jk_0\right)^{n+3}\left(n+1\right)}{\left(n+2\right)!}\left[2h^2+\left(n+1\right)x^2\right]\left(x^2+h^2\right)^{\frac{n-3}{2}}\right\}
\tag{A8}
$$

Therefore, from Eq. (A5)

$$
\begin{aligned}
T(\rho) &= -\frac{4}{j\pi k_0\zeta_0}\int_0^\rho \frac{\partial}{\partial x}\left[xE_\phi^0(x,-h)\right]\frac{1}{\sqrt{\rho^2-x^2}}\mathrm{d}x \\
&= \frac{m_z}{\pi^2}\int_0^\rho x\left\{-\frac{2h^2-x^2}{(x^2+h^2)^{5/2}}+\sum_{n=0}^\infty\frac{(-jk_0)^{n+2}(n+1)}{(n+2)!}\left[2h^2+(n+1)x^2\right]\left(x^2+h^2\right)^{\frac{n-3}{2}}\right\}\frac{1}{\sqrt{\rho^2-x^2}}\mathrm{d}x
\end{aligned}
\tag{A9}
$$

By letting $\tau = \sqrt{x^2+h^2}$ we obtain

$$
\begin{aligned}
T(\rho) = \frac{m_z}{\pi^2}\Bigg\{&-\int_h^{\sqrt{\rho^2+h^2}}\frac{3h^2-\tau^2}{\tau^4\sqrt{\rho^2+h^2-\tau^2}}\mathrm{d}\tau \\
&+\sum_{n=2}^\infty\frac{(-j)^n(n-1)}{n!a^n}(k_0a)^n\int_h^{\sqrt{\rho^2+h^2}}\frac{\left[(3-n)h^2+(n-1)\tau^2\right]}{\tau^{4-n}\sqrt{\rho^2+h^2-\tau^2}}\mathrm{d}\tau\Bigg\}
\end{aligned}
\tag{A10}
$$

The first integral in Eq. (A10) can be easily calculated: it corresponds to $T_0(\rho)$, and the computation leads again to the result in Eq. (33). In fact

$$
T_0(\rho) = \frac{m_z}{\pi^2}\int_h^{\sqrt{\rho^2+h^2}}\frac{\tau^2-3h^2}{\tau^4\sqrt{\rho^2+h^2-\tau^2}}\mathrm{d}\tau = -\frac{2m_zh\rho}{\pi^2\left(\rho^2+h^2\right)^2}
\tag{A11}
$$

It is worth noting that in Eq. (A10) the term proportional to k_0 vanishes, i.e., $T_1(\rho)=0$. The other integrals in the series (A10) are directly related to the higher-order $T_n(\rho)$ terms, i.e.,

$$
T_n(\rho) = \frac{m_z}{\pi^2}\frac{(-j)^n(n-1)}{n!a^n}\int_h^{\sqrt{\rho^2+h^2}}\frac{\left[(3-n)h^2+(n-1)\tau^2\right]}{\tau^{4-n}\sqrt{\rho^2+h^2-\tau^2}}\mathrm{d}\tau
\tag{A12}
$$

For the integrals, it results in that

$$
\int_h^{\sqrt{\rho^2+h^2}}\frac{(3-n)h^2+(n-1)\tau^2}{\tau^{4-n}\sqrt{\rho^2+h^2-\tau^2}}\mathrm{d}\tau = \int_h^{\sqrt{\rho^2+h^2}}\frac{(3-n)h^2\tau^{n-4}}{\sqrt{\rho^2+h^2-\tau^2}}\mathrm{d}\tau + \int_h^{\sqrt{\rho^2+h^2}}\frac{(n-1)\tau^{n-2}}{\sqrt{\rho^2+h^2-\tau^2}}\mathrm{d}\tau
\tag{A13}
$$

Now, by letting $\tau = \sqrt{\rho^2+h^2}\sin t$, we have

$$
\begin{aligned}
\int_h^{\sqrt{\rho^2+h^2}}\frac{(3-n)h^2+(n-1)\tau^2}{\tau^{4-n}\sqrt{\rho^2+h^2-\tau^2}}\mathrm{d}\tau = &(3-n)h^2\left(\rho^2+h^2\right)^{n/2-2}\int_{\Theta(\rho)}^{\pi/2}\sin^{n-4}t\mathrm{d}t \\
&+(n-1)\left(\rho^2+h^2\right)^{n/2-1}\int_{\Theta(\rho)}^{\pi/2}\sin^{n-2}t\mathrm{d}t
\end{aligned}
\tag{A14}
$$

where

$$
\Theta(\rho) = \sin^{-1}\left(\frac{h}{h^2+\rho^2}\right) = \tan^{-1}\frac{h}{\rho}
\tag{A15}
$$

By using

$$
\int\sin^{n-4}t\mathrm{d}t = \frac{\sin^{n-3}t\cos t}{(n-3)}+\frac{n-2}{n-3}\int\sin^{n-2}t\mathrm{d}t
\tag{A16}
$$

we obtain

$$
\int_h^{\sqrt{\rho^2+h^2}}\frac{(3-n)h^2+(n-1)\tau^2}{\tau^{4-n}\sqrt{\rho^2+h^2-\tau^2}}\mathrm{d}\tau = \frac{h^{n-1}\rho}{(\rho^2+h^2)}+\left[h^2+(n-1)\rho^2\right]\left(\rho^2+h^2\right)^{n/2-2}\int_{\Theta(\rho)}^{\pi/2}\sin^{n-2}t\mathrm{d}t
\tag{A17}
$$

The integral in Eq. (A17) has different expressions depending on if the exponent of the sine function in Eq. (A17) is even or odd [32, 2.511.2–2.511.3]. In particular, it results in

$$\int_{\Theta(\rho)}^{\pi/2} \sin^{2m} y\, dy = \frac{1}{2^{2m}} \binom{2m}{m} \left[\frac{\pi}{2} - \tan^{-1} \frac{h}{\rho} \right] - \frac{(-1)^m}{2^{2m-1}} \sum_{k=0}^{m-1} (-1)^k \binom{2m}{k} \frac{\sin \left[(2m-2k) \tan^{-1} \frac{h}{\rho} \right]}{2m-2k} \quad \text{(A18)}$$

and

$$\int_{\Theta(\rho)}^{\pi/2} \sin^{2m+1} y\, dy = -\frac{1}{2^{2m}} (-1)^{m+1} \sum_{k=0}^{m} (-1)^k \binom{2m+1}{k} \frac{\cos \left[(2m+1-2k) \tan^{-1} \frac{h}{\rho} \right]}{2m+1-2k} \quad \text{(A19)}$$

Therefore, from Eqs. (A10), (A17), and (A18)-(A19), the remaining generic expansion coefficients of the function $T(\rho)$ (i.e., for $n > 1$) can be expressed as

$$T_{2n} = \frac{m_z}{\pi^2} \frac{(-j)^{2n} (2n-1)}{(2n)! a^{2n}} \left\{ \frac{h^{2n-1}\rho}{\rho^2 + h^2} + \left[h^2 + (2n-1)\rho^2 \right] \left[\left(\rho^2 + h^2 \right)^{n-2} \frac{(2n-3)!!}{2^{n-1}(n-1)!} \left(\frac{\pi}{2} - \tan^{-1} \frac{h}{\rho} \right) \right. \right.$$
$$\left. \left. + \frac{1}{(2n-2)} \frac{\rho h^{2n-3}}{\rho^2 + h^2} + \frac{1}{(2n-2)} \sum_{k=1}^{n-2} \frac{(2n-3)(2n-5)\dots(2n-2k-1)}{2^k (n-2)(n-3)\dots(n-k-1)} \frac{\rho h^{2n-2k-3}}{\left(\rho^2 + h^2 \right)^{1-k}} \right] \right\} \quad \text{(A20)}$$

$$T_{2n+1} = \frac{m_z}{\pi^2} \frac{(-j)^{2n+1} 2n}{(2n+1)! a^{2n+1}}$$
$$\cdot \left[\frac{h^{2n}\rho}{\rho^2 + h^2} + \frac{\left(h^2 + 2n\rho^2 \right)}{2n-1} \frac{\rho h^{2n-2}}{\left(\rho^2 + h^2 \right)} + \frac{\left(h^2 + 2n\rho^2 \right)}{2n-1} \sum_{k=0}^{n-2} \frac{2^{k+1}(n-1)(n-2)\dots(n-k-1)}{(2n-3)(2n-5)\dots(2n-2k-3)} \frac{\rho h^{2n-2k-4}}{\left(\rho^2 + h^2 \right)^{-k}} \right]$$
$$\text{(A21)}$$

REFERENCES

1. Bethe, H. A., "Theory of diffraction by small holes," *Physical Review*, Vol. 66, Nos. 7–8, 163, 1944.
2. Bouwkamp, C., "On the diffraction of electromagnetic waves by small circular disks and holes," Philips Research Reports, Vol. 5, 401–422, 1950.
3. Eggimann, W., "Higher-order evaluation of dipole moments of a small circular disk," *IRE Trans. Microw. Theory Techn.*, Vol. 8, No. 5, 573–573, 1960.
4. "Higher-order evaluation of electromagnetic diffraction by circular disks," *IRE Trans. Microw. Theory Techn.*, Vol. 9, No. 5, 408–418, 1961.
5. Williams, W., "Electromagnetic diffraction by a circular disk," *Proc. Cambridge Phil. Soc.*, Vol. 58, No. 4, 625–630, Cambridge University Press, 1962.
6. Jones, D., "Diffraction at high frequencies by a circular disc," *Proc. Cambridge Phil. Soc.*, Vol. 61, No. 1, 223–245, Cambridge University Press, 1965.
7. Marsland, D., C. Balanis, and S. Brumley, "Higher order diffractions from a circular disk," *IEEE Trans. Antennas Propag.*, Vol. 35, No. 12, 1436–1444, 1987.
8. Duan, D.-W., Y. Rahmat-Samii, and J. P. Mahon, "Scattering from a circular disk: A comparative study of PTD and GTD techniques," *Proc. IEEE*, Vol. 79, No. 10, 1472–1480, 1991.
9. Nosich, A. I., "The method of analytical regularization in wave-scattering and eigenvalue problems: Foundations and review of solutions," *IEEE Antennas Propag. Mag.*, Vol. 41, No. 3, 34–49, 1999.
10. Bliznyuk, N. Y., A. I. Nosich, and A. N. Khizhnyak, "Accurate computation of a circular-disk printed antenna axisymmetrically excited by an electric dipole," *Microw. Opt. Techn. Lett.*, Vol. 25, No. 3, 211–216, 2000.
11. Bliznyuk, A. N. N. Y., "Numerical analysis of a dielectric disk antenna," *Telecommunications and Radio Engineering*, Vol. 61, 273–278, 2004.

12. Hongo, K. and Q. A. Naqvi, "Diffraction of electromagnetic wave by disk and circular hole in a perfectly conducting plane," *Progress In Electromagnetics Research*, Vol. 68, 113–150, 2007.

13. Balaban, M. V., R. Sauleau, T. M. Benson, and A. I. Nosich, "Dual integral equations technique in electromagnetic wave scattering by a thin disk," *Progress In Electromagnetics Research B*, Vol. 16, 107–126, 2009.

14. Hongo, K., A. D. U. Jafri, and Q. A. Naqvi, "Scattering of electromagnetic spherical wave by a perfectly conducting disk," *Progress In Electromagnetics Research*, Vol. 129, 315–343, 2012.

15. Di Murro, F., M. Lucido, G. Panariello, and F. Schettino, "Guaranteed-convergence method of analysis of the scattering by an arbitrarily oriented zero-thickness PEC disk buried in a lossy half-space," *IEEE Trans. Antennas Propag.*, Vol. 63, No. 8, 3610–3620, 2015.

16. Nosich, A. I., "Method of analytical regularization in computational photonics," *Radio Sci.*, Vol. 51, No. 8, 1421–1430, 2016.

17. Lucido, M., G. Panariello, and F. Schettino, "Scattering by a zero-thickness PEC disk: A new analytically regularizing procedure based on Helmholtz decomposition and Galerkin method," *Radio Sci.*, Vol. 52, No. 1, 2–14, 2017.

18. Lovat, G., P. Burghignoli, R. Araneo, S. Celozzi, A. Andreotti, D. Assante, and L. Verolino, "Shielding of a perfectly conducting circular disk: Exact and static analytical solution," *Progress In Electromagnetics Research C*, Vol. 95, 167–182, 2019.

19. "Shielding of an imperfect metallic thin circular disk: Exact and low-frequency analytical solution," *Progress In Electromagnetics Research*, Vol. 167, 1–10, 2020.

20. Saidoglu, N. Y. and A. I. Nosich, "Method of analytical regularization in the analysis of axially symmetric excitation of imperfect circular disk antennas," *Computers & Mathematics with Applications*, Vol. 79, 2872–2884, 2020.

21. Kocifaj, M., J. Klačka, F. Kundracik, and G. Videen, "Charge-induced electromagnetic resonances in nanoparticles," *Ann. Phys.*, Vol. 527, Nos. 11–12, 765–769, 2015.

22. Sneddon, I. N., *Mixed Boundary Value Problems in Potential Theory*, North-Holland Pub. Co., Amsterdam, 1966.

23. Lebedev, N. and I. Skal'skaya, "Dual integral equations and the diffraction of electromagnetic waves by a conducting plane with a slit," *Soviet Physics-Technical Physics*, Vol. 16, 1047–1054, 1972.

24. "Dual integral equations and diffraction of electromagnetic waves by a thin conducting strip," *Soviet Physics-Technical Physics*, Vol. 17, 539–545, 1972.

25. Dôme, G., E. Gianfelice, L. Palumbo, V. Vaccaro, and L. Verolino, "Longitudinal coupling impedance of a circular iris," *Il Nuovo Cimento A (1965–1970)*, Vol. 104, No. 8, 1241–1255, 1991.

26. Dôme, G., L. Verolino, L. Palumbo, and V. G. Vaccaro, "A method for computing the longitudinal coupling impedance of circular apertures in a periodic array of infinite planes," cm-P00061056, Tech. Rep., 1991.

27. Balanis, C. A., *Advanced Engineering Electromagnetics*, 2nd Edition, New York, Wiley, 1999.

28. Chew, W. C., *Waves and Fields in Inhomogenous Media*, IEEE Press, Piscataway, NJ, 1999.

29. Van Bladel, J., *Singular Electromagnetic Fields and Sources*, Clarendon Press, Oxford, UK, 1991.

30. Dudley, D. G., *Mathematical Foundations for Electromagnetic Theory*, IEEE Press, Piscataway, NJ, 1994.

31. Poularikas, A. D., *Handbook of Formulas and Tables for Signal Processing*, 2nd Edition, CRC Press, Boca Raton, FL, 1998.

32. Gradshteyn, I. S. and I. M. Ryzhik, *Table of Integrals, Series, and Products*, 7th edition, Academic Press, Burlington, MA, 2014.